Nanoscale

Accepted Manuscript

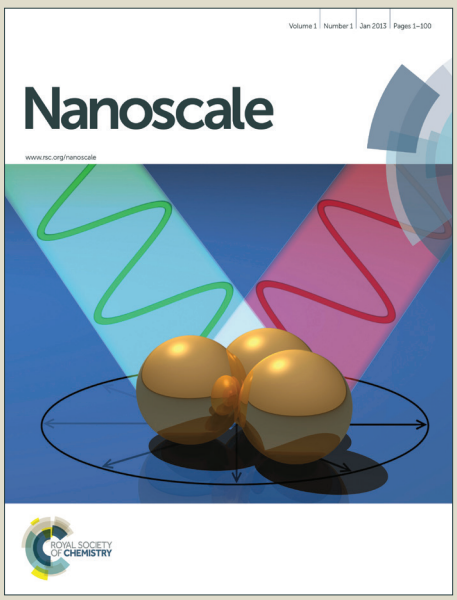

ROYAL SOCIETY OF CHEMISTRY

www.rsc.org/nanoscale

Unusual effects of solvent polarity on capacitance for organic electrolytes in a nanoporous electrode

De-en Jiang*[a] and Jianzhong Wu*[b]

[a]*Chemical Sciences Division, Oak Ridge National Laboratory, Oak Ridge, Tennessee, 37831*

[b]*Department of Chemical and Environmental Engineering, University of California, Riverside, California 92521*

*Corresponding authors. E-mail: jiangd@ornl.gov and jwu@engr.ucr.edu.

Abstract

Interplay between ions and solvent molecules inside the nanoporous electrodes of a supercapacitor has not been well understood but could be a fertile ground for new insights into the device performance. By tuning the dipole moment of the solvent in an organic electrolyte, we find from classical density functional theory calculations pronounced oscillation of capacitance with the pore size for a moderately to weakly polar solvent. A quantitative analysis of the electric-double-layer (EDL) structure indicates that the capacitance oscillation shares a similar physical origin as that in an ionic-liquid electrolyte: the oscillatory behavior arises from the formation of alternating layers of counterions and coions near strongly charged surfaces. More interestingly, we find that, in the large-pore region, the capacitance versus the pore size has a volcano shape; in other words, there exists a solvent dipole moment that yields a maximal capacitance. These theoretical predictions can be validated with future experiments and highlight the great potential in tuning the organic solvent to achieve optimal performance of EDL capacitors.

Introduction

Electric-double-layer capacitors (EDLCs), also known as supercapacitors, have the advantages of high power density, fast charging time (in seconds), and long cycling lifespan (up to millions of charge-discharge cycles) in comparison to batteries,[1-3] making them increasingly attractive for energy storage in transportation applications, such as in hybrid buses and regenerative breaking. On the fundamental side, tuning the pore size,[4-6] surface area,[7] morphology,[8-11] architecture,[12, 13] and functionality[14, 15] of the electrode materials as well as exploring the diversity of the electrolytes[16-18] have yielded new insights into the rich electrochemical behavior of electrolytes inside porous electrodes. Among many scientific issues related to the electrode/electrolyte interface and electrolytes in porous electrodes, the question how the surface-area-normalized capacitance of an EDLC changes with the pore size has been pursued by both experimental[4, 5, 19] and theoretical means.[20-30]

From the "anomalous increase" of capacitance[4, 31] to "flat pattern"[19] to long-range oscillation[23, 26, 28] and from desolvation[31] to the "superionic state"[29] to the EDL interference,[23, 25, 26] it seems that a consensus has been reached that the capacitance does increase significantly as the pore size of the electrode shrinks to the ionic dimensions. What is more interesting is how the capacitance changes progressively as the pore size increases from one to multiple times of the ionic diameter. Classical density functional theory (CDFT) predicted that the capacitance of a slit-pore electrode would oscillate with the pore size at a periodicity of ~1.4 times the ion diameter of the ionic-liquid electrolyte.[23, 25] The amplitude of the oscillation is damped as the pore size increases and becomes negligible when it is beyond about nine times the ion diameter. The first two peaks of the oscillation have also been shown independently from all-atom molecular dynamics simulations.[26, 28]

For a model electrolyte such as tetraethylammonium tetrafluoroborate (TEA-BF4) dissolved a strongly polar solvent, CDFT predicts a relatively flat curve on the pore-size dependence of the capacitance when the pore size is larger than two times the ion diameter.[24] An important question is whether this behavior is generally valid given the diversity of organic electrolytes in EDLCs.[32-43] Specifically, how would the solvent properties such as the polarity affect the capacitance dependence on the pore size? And is there an optimal dipole moment for a given porous electrode? In this paper, we will address these questions using CDFT and show that an organic electrolyte capacitor displays rich behavior sensitive to the polarity of the solvent.

Model and method

We consider a model supercapacitor as shown in Figure 1 where a positive potential of 1.5V relative to that of the bulk electrolyte is applied to the confining walls of the porous electrode represented by a slit pore. The confined electrolyte can exchange ions and solvents with a reservoir of the bulk electrolyte. Due to the symmetric nature of the EDLC electrodes (namely, both electrodes are the same material), the negative electrode will be at -1.5 V relative to the bulk value, yielding a voltage window of 3.0 V, close to the commonly applied voltages for the non-aqueous electrolytes (2.3 – 2.7 V). For simplicity, the ions are modeled as charged hard spheres of 0.5 nm in diameter; the solvent molecules are tangentially connected dimers of hard spheres with opposite charges. The size of each monomer of the solvent molecule is fixed at 0.3 nm in diameter, while the polarity or the dipole moment is tuned by changing the monomeric charges. The organic nature of the solvent is represented by the variation in the dipole moment. In all theoretical calculations, the salt concentration in the bulk is fixed at 1.5 M at 298 K, as used in the experiment.[4] Since the cation and the anion are of the same size in our model system,

the simulation results will be symmetric between the positive and negative electrodes. In other words, we only need to simulate a single electrode for one type of applied potentials (such as a positive potential); the exchange of ions and solvents with the reservoir can be handled using the grand canonical ensemble.[44]

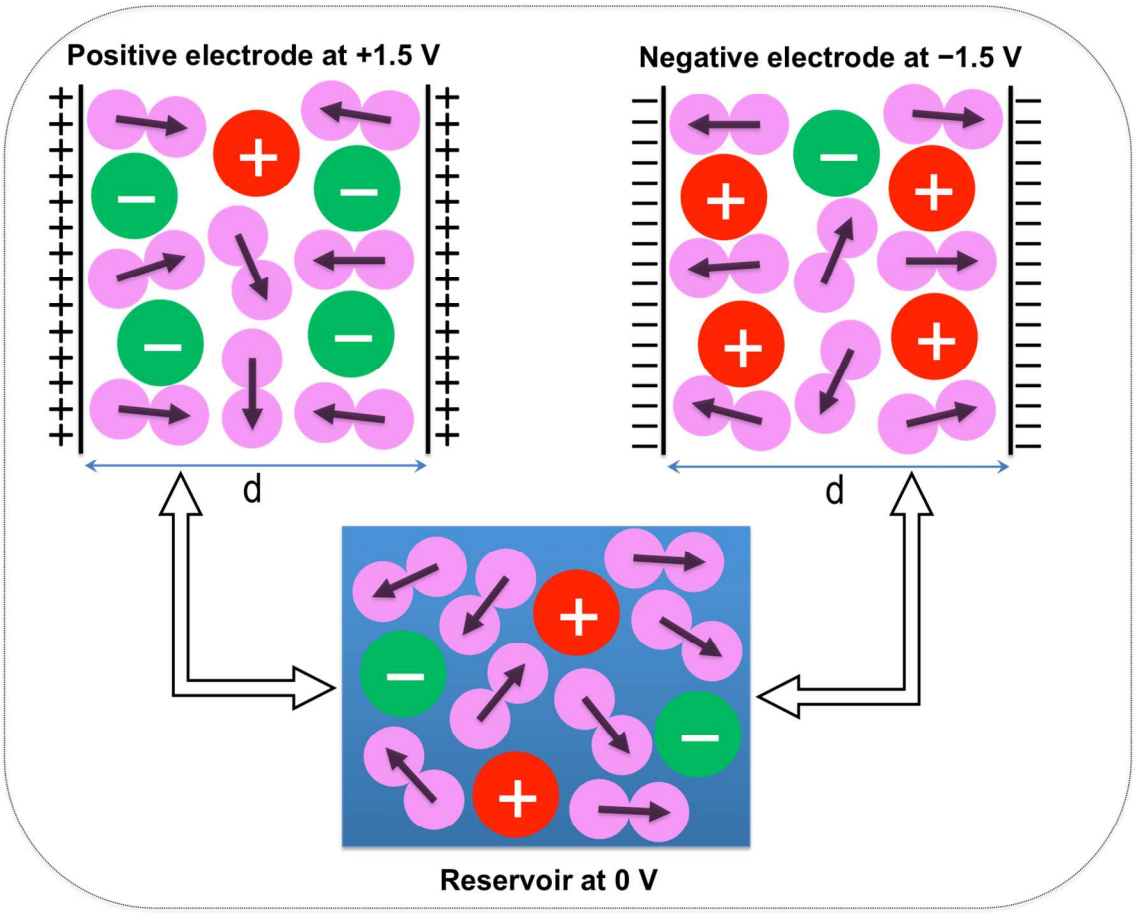

Figure 1. A model supercapacitor mimicking an organic electrolyte in porous electrodes: a slit pore of width *d* is used to represent the positive and negative electrodes and the confined electrolyte is in equilibrium with a bulk reservoir (See text for detailed explanation).

Given the reservoir electrolyte (1.5 M at 298 K for a solvent of a specific dipole moment), the pore width (for example, d =1.0 nm), and the applied potential (U=1.5 V), we calculated the density profiles of cations, anions, and solvent molecules self-consistently by minimizing the

free energy of the system. From the converged density profiles of ions inside the single electrode, we can obtain the electrode surface charge density (Q) according to macroscopic charge neutrality. The integral capacitance is simply determined as $C = Q/U$ (where U is 1.5 V in our case), since the electrode potential at the point of zero charge is zero due to the symmetric cation and anion used in our model setup (Figure 1). For a detailed explanation of the CDFT method, we refer the reader to our previous papers.[23-25, 45, 46] Compared with the all-atom molecular dynamics simulation, coarse-grained CDFT is much more computationally efficient and usually one simulation can be finished within a couple of days on a single processor. Therefore, it allows one to explore many pore sizes leading to a large size. In contrast, all-atom MD simulation is much slower and usually one simulation takes weeks to months to finish on a supercomputer or a computer cluster. Due to this limitation, all-atom MD simulation can explore only a few small pore sizes.[26, 28] Of course, all-atom MD simulation can provide much more atomic detail in terms of interaction at the electrode/electrolyte interface, but the coarse-grained model is sufficient for the purpose of the present work to address the capacitance vs. pore size relationship in organic-electrolyte EDLCs of various polarity.

Results and discussion

Our theoretical investigations are directed at examining two parameters on the capacitance: (i) the pore width d and (ii) the solvent dipole moment. Figure 2 shows how the capacitance changes with the pore size for the model EDLC with an organic electrolyte of different solvent dipole moments. Here the most polar solvent has a dipole moment of 3.40 Debye, slightly smaller than that for acetonitrile (3.91 Debye).[47] As the polarity decreases from 3.40 Debye to 2.55 Debye (close to the dipole moment of acetone which is 2.88 Debye[48]), one sees little change

in the basic features on the pore-size dependence of the capacitance: the curve shows a large peak at 0.5 nm (the ion diameter), a trough at 0.75 nm, and a more-or-less flat curve beyond 1.0 nm. However, as the solvent dipole moment is further decreased from 2.55 Debye to 1.70 Debye (close to the dipole moment of tetrahydrofuran, which is 1.75 Debye[48]), a qualitatively different picture emerges. The capacitance now oscillates with the pore size in a way intimately reminiscent of what was observed for ionic-liquid supercapacitors.[23] To our knowledge, this is the first prediction of capacitance oscillation for an organic electrolyte supercapacitor. When the dipole moment of the solvent is lowered to 0.85 Debye, we see that the capacitance oscillation is further enhanced, as indicated by the greater amplitudes.

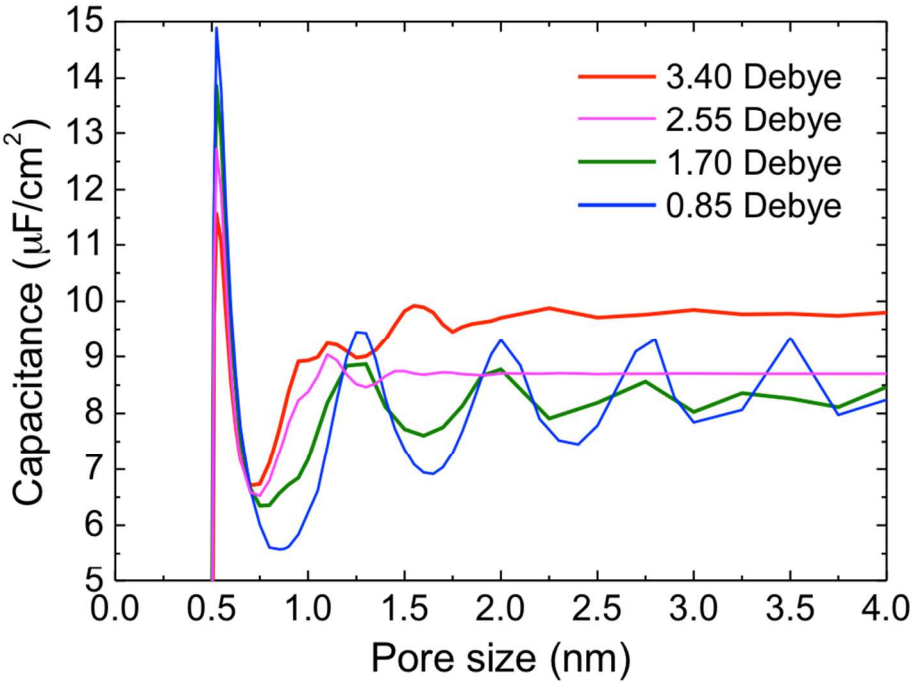

Figure 2. Integral capacitance (at 1.5V relative to the bulk electrolyte) versus the pore size for several organic electrolytes of different polarities. Different lines correspond to solvents with different dipole moments.

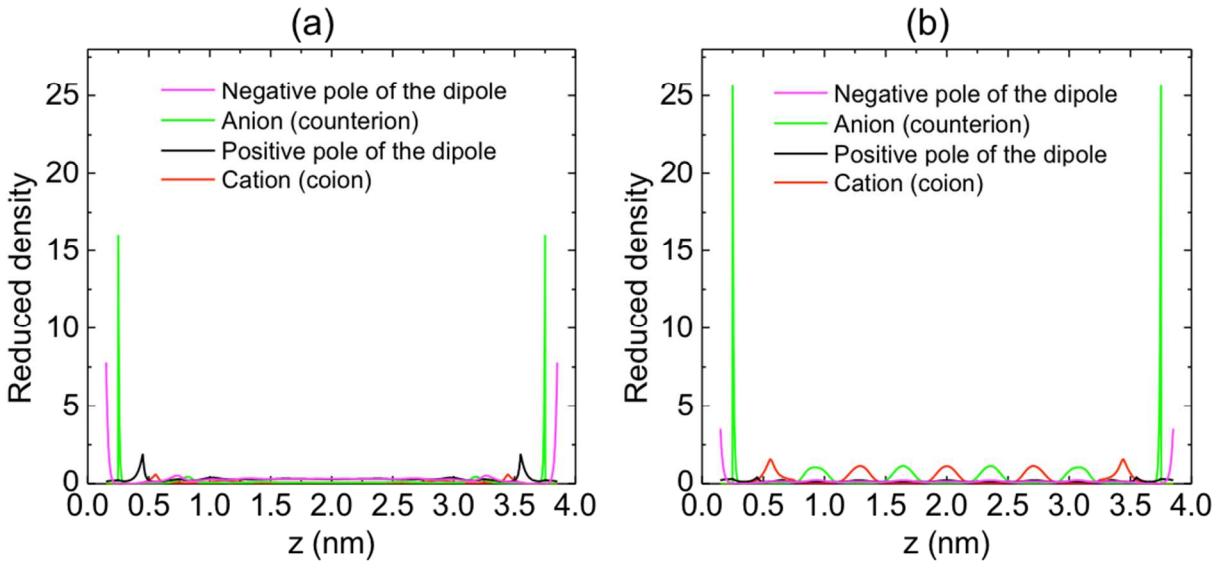

Figure 3. Reduced density profiles of cations, anions, and the solvent segments inside a 4.0-nm slit pore at 1.5V surface potential: (a) 2.55 Debye; (b) 1.70 Debye. The two positively charged walls are positioned at z=0 and z=4 nm, respectively. Reduced density for an ion or segment is defined as $\rho\sigma^3$, where ρ and σ are the number density and diameter of the ion or the segment, respectively.

What causes the capacitance oscillation when the solvent polarity is reduced? To answer this question, we analyzed the EDL structure inside a 4.0-nm slit pore. In this case, there is little interaction between the EDLs from the opposite walls. Figure 3a shows the reduced density profiles for the organic electrolyte with the 2.55-Debye solvent. One can see that the EDL is dominated by a contact layer of counterions (green peak in Figure 3a) and aligned dipoles (pink and black peaks in Figure 3a). The picture is similar to what we observed for the supercapacitor with a 3.4-Debye solvent.[24] Beyond the contact layer, the ionic densities show little change with the distance from the surface.

Next we analyze the system with a solvent of 1.70 Debye dipole moment (Figure 3b). One distinctive feature of this system is that cations and anions form alternating layers inside the pore, while the solvent density is negligible beyond the contact layers. Although the layered structures

next to a charged surface have been well documented at the ionic liquid/electrode interface,[45, 49] no previous report indicates that such behavior can also happen for an organic electrolyte inside a slit pore. We also analyzed the EDL structure of the organic electrolyte with the 0.85-Debye solvent and found that the density profiles of ions and the solvent dipoles are similar to those of the system with the 1.70-Debye solvent.

Because of the similarity in the pore-size dependence of the capacitance behavior, it would be instructive to compare the oscillatory patterns between the organic electrolyte and an ionic liquid.[23] We found that the degree of capacitance oscillation for the organic electrolyte with the 1.70-Debye solvent matches very well that of the ionic liquid (Figure 4). This is a very interesting comparison given the great similarity in terms of peak positions and amplitudes of the oscillation between the two electrolytes. One way to understand this similarity is that, as we reduce the dipole moment of the solvent, solvent molecules are excluded from the slit pore so that the organic electrolyte behaves like an ionic liquid: cations and anions form alternating layers near the charged surfaces and the interference of the ionic layers leads to capacitance oscillation.[23, 25] What is unique with the organic solvent is that the degree of the oscillation can be further enhanced by tuning the dipole moment of the solvent, as shown in Figure 2. This enhancement is caused by the relative tendency to drive ions into the pore: When the dipole moment of the solvent is further weakened, the ions now have a higher tendency to go into the pore and form layered structures that lead to even stronger capacitance oscillation. Indeed, the EDL structure for the 0.85-Debye solvent displays alternating layers of cations and anions of higher densities in the pore than those of the 1.70-Debye solvent.

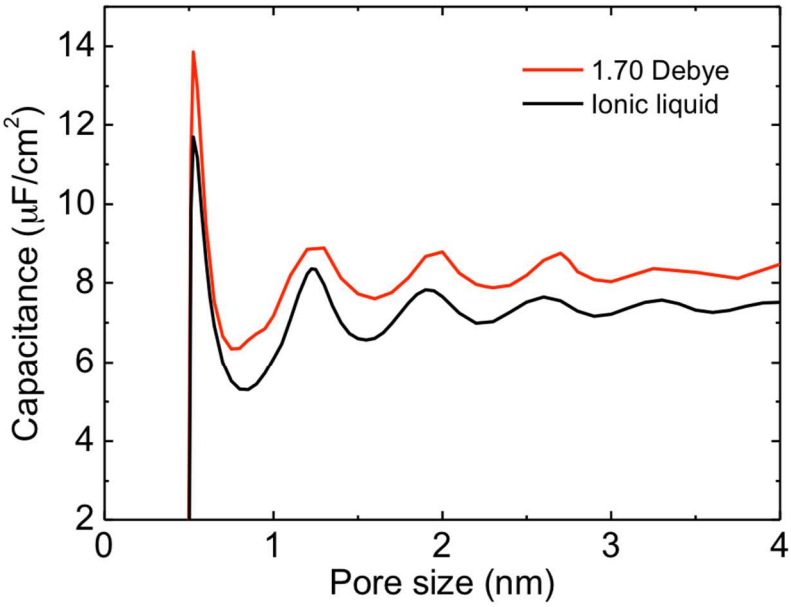

Figure 4. Comparison of integral capacitance (at 1.5V relative to the bulk electrolyte) versus the pore size between an organic electrolyte with a 1.70-Debye solvent (Figure 1) and an ionic liquid.[23]

Now that we have shown that the capacitance may oscillate for an organic electrolyte when the dipole moment of the solvent is below a certain value, the next question is how the capacitance varies with the pore size for strongly polar solvents. To address this question, we consider systems with solvent dipole moment larger than 3.40 Debye, given that a popular solvent such as acetonitrile has a dipole moment of 3.91 Debye.[47] Figure 5 presents the case of an organic electrolyte with a solvent molecule of the 4.50-Debye dipole moment, which is between those of acetonitrile and propylene carbonate (4.9 Debye) − another popular solvent for EDLCs. Although the overall picture is similar between the 3.40-Debye and 4.50-Debye electrolytes, two distinctive features stand out: (a) the first peak at 0.5nm (the ion diameter) is in fact not corresponding to the capacitance maximum any more; (b) the capacitance maximum occurs at 1.5 nm, three times the ion diameter.

To understand this abnormal behavior, we again examine the EDL structure of ions and the dipoles inside the 1.5nm slit pore for the 4.50-Debye solvent (Figure 6a). We observe that the EDL structure is now in fact dominated by the aligned dipoles (pink peak at 0.15 nm and black peak at 0.45 nm) and that the density of counterions (green peak at 0.25 nm) next to the charged wall is less than one third of the negative pole of the dipole. More interestingly, there is a minor amount of dipoles that are anti-aligned against the wall (black peak at 0.15 nm and pink peak at 0.45 nm). Figure 6b shows a cartoonish picture of the main features of the EDL structure. These anti-aligned dipoles consist of a new feature for the 4.50-Debye solvent, since they are absent for the 3.40-Debye solvent.

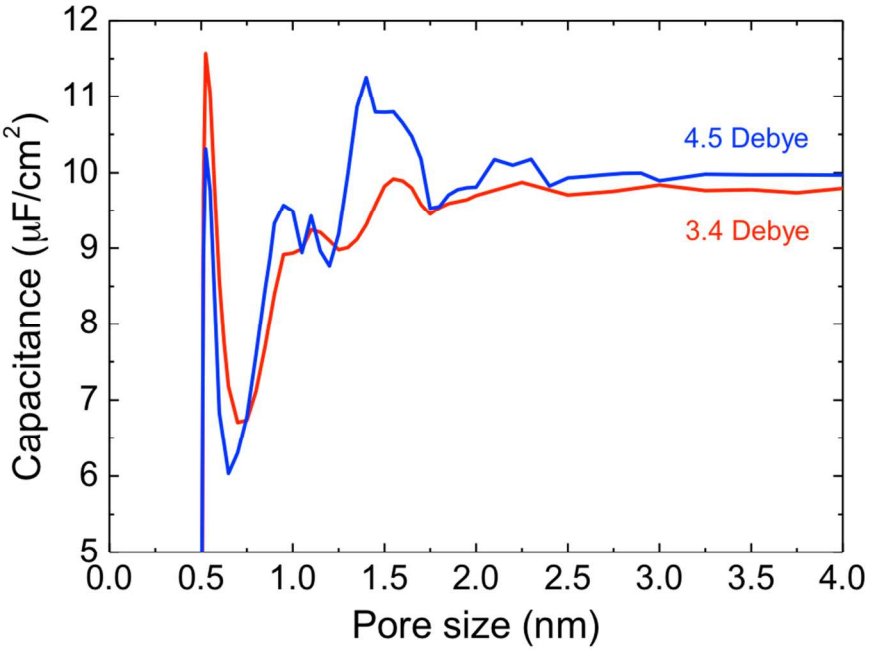

Figure 5. Integral capacitance (at 1.5V relative to the bulk electrolyte) versus the pore size for organic electrolytes of different solvent polarity: 3.4 Debye vs. 4.5 Debye.

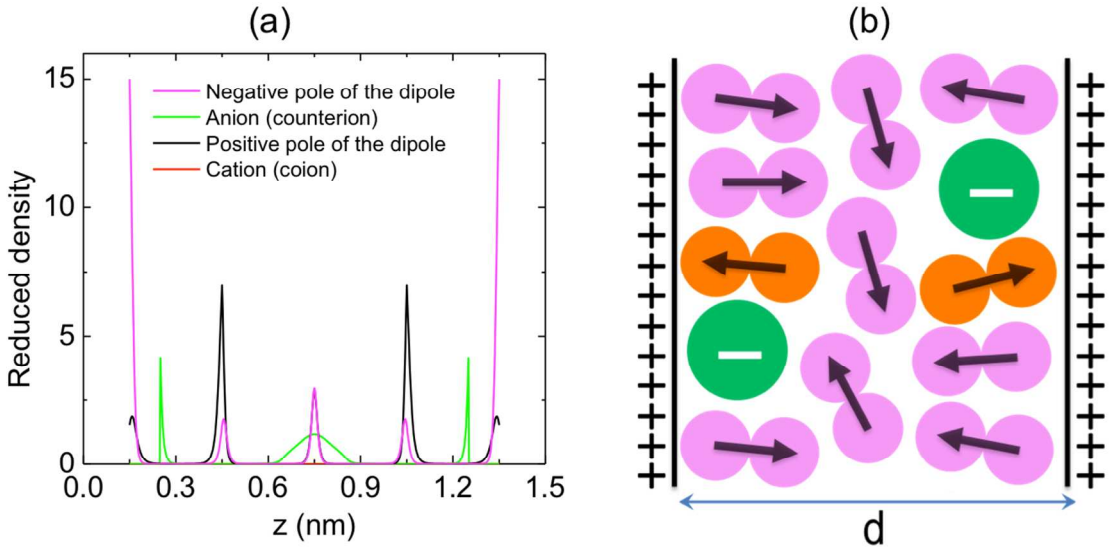

Figure 6. (a) Reduced density profiles of cations, anions, and the solvent segments inside the 1.5-nm slit pore at 1.5V surface potential for the organic electrolyte with a dipolar solvent of 4.5 Debye. The two positively charged walls are at z=0 and z=1.5 nm. (b) A cartoonish picture to show the main features of the EDL structure, with the anti-aligned dipoles labeled in orange.

Figure 5 shows that, for the system with the solvent dipole moment of 4.5 Debye, the capacitance becomes relatively insensitive to the pore size beyond certain range and its value at the asymptotic limit is comparable to that for the first peak where the pore size approaches the ionic dimension. Hence it would be interesting to examine how this asymptotic limit (for example, the capacitance at 4.0 nm) depends on the dipole moment of the solvent. The results from the DFT predictions are plotted in Figure 7a, which shows, surprisingly, a volcano shape as the dipole moment varies from 2.5 to 5 Debye. The capacitance first increases with the solvent dipole moment, reaches a maximum at about 4.0 Debye, and then decreases.

Why is there such a volcano shape? It certainly results from the interplay of ions and solvent molecules confined in the nanoporous electrode and may be understood as follows. As the solvent varies from weak-to-moderate polarity, more solvent molecules enter the slit pore and the

majority of them are aligned against the charged wall together with the counterions (Figure 3a). Due to the smaller size of the solvent segments than the counterions (see Figure 6b), the presence of the solvent molecules leads to a smaller effective distance of the layer of the oppositely charged mobile ions (negative poles and anions in Figure 6b) to the charged wall, hence a larger capacitance. At the peak-position dipole moment (4.0 Debye), about 50% of the counterions (anions) and 80% of the coions (cations) are excluded from the pore in comparison with those of the 3.4 Debye case (Figure 7b). When the dipole moment is further increased, the strong polarity of the solvent now leads to a reduction of the net charges in the slit pore (namely, further expulsion of counterions while the amount of coions already reduced to negligible), hence a smaller capacitance. In short, it is the interplay between ions and solvent molecules at the charged electrode surface that leads to the volcano shape in Figure 7a. How general this shape is for other situations (such as different pore geometry and more realistic solvents and salts) remains to be explored. We hope that more advanced CDFT models or all-atom molecular dynamics simulations would answer this question in the near future.

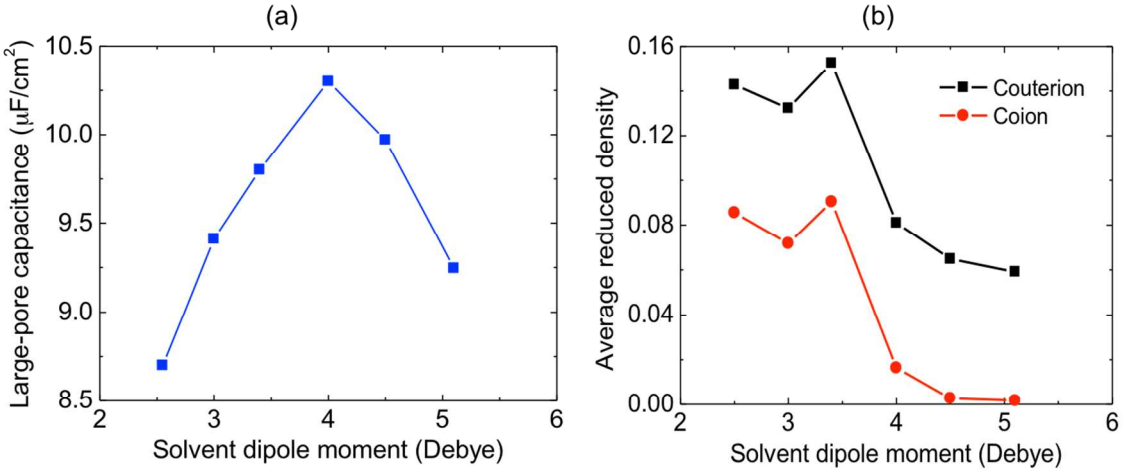

Figure 7. (a) Integral capacitance (at 1.5V relative to the bulk electrolyte) of an organic electrolyte in a 4.0-nm pore versus the solvent dipole moment; (b) the average reduced densities of counterions and coions inside the 4.0-nm pore with 1.5 V surface potential.

Whereas there have been many theoretical studies on the applications of ionic liquids for EDLCs,[6, 22, 23, 27, 29, 50-54] relatively few publications have been devoted to organic electrolytes[41, 43, 55, 56] despite the fact that the latter is broadly employed in commercial supercapacitors. In this work we have shown that the interplay between solvents and ions inside a nanopore may result in very rich electrochemical behavior, adding to the already many experimental findings and recent computational insights about organic electrolytes in EDLCs.[32-43] Despite the simplicity or ideality of the model systems, the dipole moments of many organic solvents used in EDLCs actually fall right into the range we considered in this work. For example, propylene carbonate has a dipole moment of 4.9 Debye, sulfolane 4.8 Debye, γ-butyrolactone 4.27 Debye, dimethylsulfoxide (DMSO) 3.96 Debye, and acetonitrile 3.91 Debye.[48] Interestingly, the latter three solvents have dipole moments at the top of the volcano plot in Figure 7a. Of course, one has to consider the salt and also the electrode material in addition to the solvent when discussing the capacitance of an EDLC. Nevertheless, the present theoretical results suggest that there indeed seems to be a range of optimal dipole moments for the organic solvent when all other things (the salt and the electrode material) being equal.

In the present coarse-grained CDFT approach the polarity of the solvent is varied by the molecular dipole moment for their theoretical convenience, in order to precisely control the input parameter and obtain a qualitative trend of capacitance versus polarity. There are other commonly used approaches to classify solvent's polarity, such as the macroscopic dielectric constants. The microscopic dipole moments and the macroscopic dielectric constants for polar liquids are related by the Onsager equation and the Kirkwood extension, and recent developments show a very good empirical correlation between the dielectric constants and the

molecular properties including the dipole moment as a leading term.[57] For the range of dipole moments we are interested here (2.5 to 5 Debye), the dielectric constants are in the range of 21 to 64, namely, moderately to strongly polar. For example, acetone has a dipole moment of 2.88 Debye and a dielectric constant of 21; acetonitrile, 3.91 Debye and 38; γ-butyrolactone, 4.27 Debye and 42; propylene carbonate, 4.9 Debye and 64.[48, 58]

One more thing to note here is that our model electrolyte provides no atomic details and the pore model is only one-dimensional. To be able to treat the real electrolytes and the real porous materials, more advanced models have to be developed for both the electrolytes and the electrode materials. From the perspective of the classical DFT method, one still needs to develop the numerical techniques to treat a multidimensional model, which is worthy of substantial efforts given the efficiency and attractiveness of the CDFT method.

Summary and conclusions

To sum up, we have explored from the classical density functional theory the capacitance dependence of the pore size for the electric-double-layer capacitors with an organic electrolyte – a salt dissolved in a polar organic solvent. By tuning the dipole moment of the solvent molecules, we have shown that the capacitance variation with the pore size may exhibit an oscillatory pattern when the polarity of the solvent is reduced below a certain value. This new prediction for an organic electrolyte of moderate to weak polarity resembles what was found for ionic liquid supercapacitors. A quantitative analysis of the EDL structure of these less polar organic electrolytes showed that the cations and anions form alternating layers against the charged walls inside the slit pore. Analogous to the ionic liquid, interference of these alternating layers leads to capacitance oscillation. For more polar solvents, we found that the maximum capacitance shifts

away from the first peak at the pore size of the ion diameter to a pore size several times the ion diameter. This shift is accompanied by an EDL structure now dominated by the solvent dipoles – most of them aligned and some anti-aligned against the charged walls. More interestingly, we found that there exists an optimal dipole moment that yields a maximum in the large-pore capacitance. Our work here illustrates rich behavior of the organic electrolytes inside porous electrodes and suggests new experiments for selecting organic electrolytes for EDLCs.

Acknowledgements

This work was supported by the Fluid Interface Reactions, Structures, and Transport (FIRST) Center, an Energy Frontier Research Center funded by the U.S. Department of Energy (DOE), Office of Science, Office of Basic Energy Sciences.

References

1. J. R. Miller and P. Simon, *Science*, 2008, **321**, 651.

2. P. Simon and Y. Gogotsi, *Nat. Mater.*, 2008, **7**, 845.

3. P. Simon and Y. Gogotsi, *Accounts Chem. Res.*, 2013, **46**, 1094.

4. J. Chmiola, G. Yushin, Y. Gogotsi, C. Portet, P. Simon and P. L. Taberna, *Science*, 2006, **313**, 1760.

5. C. Largeot, C. Portet, J. Chmiola, P. L. Taberna, Y. Gogotsi and P. Simon, *J. Am. Chem. Soc.*, 2008, **130**, 2730.

6. S. Kondrat, C. R. Perez, V. Presser, Y. Gogotsi and A. A. Kornyshev, *Energy Environ. Sci.*, 2012, **5**, 6474.

7. Y. W. Zhu, S. Murali, M. D. Stoller, K. J. Ganesh, W. W. Cai, P. J. Ferreira, A. Pirkle, R. M. Wallace, K. A. Cychosz, M. Thommes, D. Su, E. A. Stach and R. S. Ruoff, *Science*, 2011, **332**, 1537.

8. J. Chmiola, C. Largeot, P. L. Taberna, P. Simon and Y. Gogotsi, *Science*, 2010, **328**, 480.

9. M. F. El-Kady, V. Strong, S. Dubin and R. B. Kaner, *Science*, 2012, **335**, 1326.

10. X. W. Yang, C. Cheng, Y. F. Wang, L. Qiu and D. Li, *Science*, 2013, **341**, 534.

11. P. X. Li, C. Y. Kong, Y. Y. Shang, E. Z. Shi, Y. T. Yu, W. Z. Qian, F. Wei, J. Q. Wei, K. L. Wang, H. W. Zhu, A. Y. Cao and D. H. Wu, *Nanoscale*, 2013, **5**, 8472.

12. C. Z. Yuan, B. Gao, L. F. Shen, S. D. Yang, L. Hao, X. J. Lu, F. Zhang, L. J. Zhang and X. G. Zhang, *Nanoscale*, 2011, **3**, 529.

13. C. Li and G. Q. Shi, *Nanoscale*, 2012, **4**, 5549.

14. L.-F. Chen, X.-D. Zhang, H.-W. Liang, M. Kong, Q.-F. Guan, P. Chen, Z.-Y. Wu and S.-H. Yu, *ACS Nano*, 2012, **6**, 7092.

15. J. Wei, D. Zhou, Z. Sun, Y. Deng, Y. Xia and D. Zhao, *Adv. Funct. Mater.*, 2013, **23**, 2322.

16. A. Janes, H. Kurig, T. Romann and E. Lust, *Electrochem. Commun.*, 2010, **12**, 535.

17. R. Y. Lin, P. L. Taberna, S. Fantini, V. Presser, C. R. Perez, F. Malbosc, N. L. Rupesinghe, K. B. K. Teo, Y. Gogotsi and P. Simon, *J. Phys. Chem. Lett.*, 2011, **2**, 2396.

18. A. Brandt, C. Ramirez-Castro, M. Anouti and A. Balducci, *J. Mater. Chem. A*, 2013, **1**, 12669.

19. T. A. Centeno, O. Sereda and F. Stoeckli, *Phys. Chem. Chem. Phys.*, 2011, **13**, 12403.

20. J. S. Huang, B. G. Sumpter and V. Meunier, *Angew. Chem.-Int. Edit.*, 2008, **47**, 520.

21. J. S. Huang, B. G. Sumpter and V. Meunier, *Chem.-Eur. J.*, 2008, **14**, 6614.

22. Y. Shim and H. J. Kim, *ACS Nano*, 2010, **4**, 2345.

23. D. E. Jiang, Z. H. Jin and J. Z. Wu, *Nano Lett.*, 2011, **11**, 5373.

24. D. E. Jiang, Z. H. Jin, D. Henderson and J. Z. Wu, *J. Phys. Chem. Lett.*, 2012, **3**, 1727.

25. D. E. Jiang and J. Z. Wu, *J. Phys. Chem. Lett.*, 2013, **4**, 1260.

26. G. Feng and P. T. Cummings, *J. Phys. Chem. Lett.*, 2011, **2**, 2859.

27. G. Feng, S. Li, V. Presser and P. T. Cummings, *J. Phys. Chem. Lett.*, 2013, **4**, 3367.

28. P. Wu, J. Huang, V. Meunier, B. G. Sumpter and R. Qiao, *ACS Nano*, 2011, **5**, 9044.

29. S. Kondrat, N. Georgi, M. V. Fedorov and A. A. Kornyshev, *Phys. Chem. Chem. Phys.*, 2011, **13**, 11359.

30. S. Kondrat, A. Kornyshev, F. Stoeckli and T. A. Centeno, *Electrochem. Commun.*, 2013, **34**, 348.

31. J. Chmiola, C. Largeot, P. L. Taberna, P. Simon and Y. Gogotsi, *Angew. Chem.-Int. Edit.*, 2008, **47**, 3392.

32. T. Morimoto, K. Hiratsuka, Y. Sanada and K. Kurihara, *J. Power Sources*, 1996, **60**, 239.

33. K. Xu, M. S. Ding and T. R. Jow, *J. Electrochem. Soc.*, 2001, **148**, A267.

34. D. Lozano-Castello, D. Cazorla-Amoros, A. Linares-Solano, S. Shiraishi, H. Kurihara and A. Oya, *Carbon*, 2003, **41**, 1765.

35. R. J. Chen, F. Wu, H. Y. Liang, L. Li and B. Xu, *J. Electrochem. Soc.*, 2005, **152**, A1979.

36. K. Y. Tse, L. Z. Zhang, S. E. Baker, B. M. Nichols, R. West and R. J. Hamers, *Chem. Mat.*, 2007, **19**, 5734.

37. F. Wu, R. J. Chen, F. Wu, L. Li, B. Xu, S. Chen and G. Q. Wang, *J. Power Sources*, 2008, **184**, 402.

38. R. Mysyk, E. Raymundo-Pinero and F. Beguin, *Electrochem. Commun.*, 2009, **11**, 554.

39. A. Lewandowski, A. Olejniczak, M. Galinski and I. Stepniak, *J. Power Sources*, 2010, **195**, 5814.

40. T. Ohta, I. T. Kim, M. Egashira, N. Yoshimoto and M. Morita, *J. Power Sources*, 2012, **198**, 408.

41. Y. Shim, H. J. Kim and Y. Jung, *Faraday Discuss.*, 2012, **154**, 249.

42. C. Zheng, M. Yoshio, L. Qi and H. Y. Wang, *J. Power Sources*, 2012, **220**, 169.

43. T. Ohba and K. Kaneko, *J. Phys. Chem. C*, 2013, **117**, 17092.

44. D. Frenkel and B. Smit, *Understanding Molecular Simulation*, Academic Press, San Diego, USA, 2002.

45. J. Z. Wu, T. Jiang, D. E. Jiang, Z. H. Jin and D. Henderson, *Soft Matter*, 2011, **7**, 11222.

46. D. E. Jiang, D. Meng and J. Z. Wu, *Chem. Phys. Lett.*, 2011, **504**, 153.

47. P. A. Steiner and W. Gordy, *J. Mol. Spectrosc.*, 1966, **21**, 291.

48. D. R. Lide, in *CRC Handbook of Chemistry and Physics*, ed. W. M. Haynes, Taylor and Francis Group, Boca Raton, FL, 94th edn., 2013, p. 9/51.

49. S. Perkin, *Phys. Chem. Chem. Phys.*, 2012, **14**, 5052.

50. C. Merlet, B. Rotenberg, P. A. Madden, P. L. Taberna, P. Simon, Y. Gogotsi and M. Salanne, *Nat. Mater.*, 2012, **11**, 306.

51. C. Merlet, B. Rotenberg, P. A. Madden and M. Salanne, *Phys. Chem. Chem. Phys.*, 2013, **15**, 15781.

52. J. Vatamanu, L. Cao, O. Borodin, D. Bedrov and G. D. Smith, *J. Phys. Chem. Lett.*, 2011, **2**, 2267.

53. L. Xing, J. Vatamanu, O. Borodin and D. Bedrov, *J. Phys. Chem. Lett.*, 2013, **4**, 132.

54. P. Wu, J. Huang, V. Meunier, B. G. Sumpter and R. Qiao, *J. Phys. Chem. Lett.*, 2012, **3**, 1732.

55. G. Feng, J. Huang, B. G. Sumpter, V. Meunier and R. Qiao, *Phys. Chem. Chem. Phys.*, 2010, **12**, 5468.

56. C. Merlet, M. Salanne, B. Rotenberg and P. A. Madden, *Electrochim. Acta*, 2013, **101**, 262.

57. J.-P. Liu, W. V. Wilding, N. F. Giles and R. L. Rowley, *J. Chem. Eng. Data*, 2009, **55**, 41.

58. C. Wohlfarth, in *CRC Handbook of Chemistry and Physics*, ed. W. M. Haynes, Taylor and Francis Group, Boca Raton, FL, 94th edn., 2013, p. 6/187.